Improved Regularized Reconstruction for Simultaneous Multi-Slice Cardiac MRI T_1 Mapping

Ömer Burak Demirel[1,2], Sebastian Weingärtner[1,2,3], Steen Moeller[2] and Mehmet Akçakaya[1,2]
[1]Department of Electrical and Computer Engineering, University of Minnesota, Minneapolis, MN
[2]Center for Magnetic Resonance Research, University of Minnesota, Minneapolis, MN
[3]Department of Imaging Physics, Delft University of Technology, Delft, Netherlands
Emails: {demir035, sweingae, moell018, akcakaya}@umn.edu

***Abstract*—Myocardial T_1 mapping is a quantitative MRI technique that has found great clinical utility in the detection of various heart disease. These acquisitions typically require three breath-holds, leading to long scan durations and patient discomfort. Simultaneous multi-slice (SMS) imaging has been shown to reduce the scan time of myocardial T_1 mapping to a single breath-hold without sacrificing coverage, albeit at reduced precision. In this work, we propose a new reconstruction strategy for SMS imaging that combines the advantages of two different k-space interpolation strategies, while allowing for regularization, in order to improve the precision of accelerated myocardial T_1 mapping.**

***Index Terms*—magnetic resonance imaging, parallel imaging, accelerated MRI**

I. INTRODUCTION

Magnetic resonance imaging (MRI) offers various soft tissue contrasts by using different magnetization relaxation processes (e.g. T_1 and T_2 relaxation). Such relaxation processes can be quantified in a pixel-wise manner to provide protocol-independent information [1, 2]. Among such quantitative MRI methods, T_1 mapping has found great clinical utility in cardiac MRI in the management of various cardiomyopathies [3].

In myocardial T_1 mapping, for a given slice, multiple images are acquired with different T_1 weights, which are used to estimate the quantitative relaxation parameters using a parametric model [4]. Typical clinical applications require three slices covering the myocardium, where each slice is acquired in a separate breath-hold [4]. Multiple breath-holds lengthen the scan time due to rest periods between each breath-held acquisition. Furthermore, they are often challenging for patients, who have difficulty breath-holding.

Simultaneous multi-slice (SMS) or multiband (MB) imaging is an image acceleration technique, where multiple slices are excited and acquired at the same time [5]. The information from these multiple slices are resolved using the redundancies among the multiple sensors in the receiver coil arrays used in MRI. An advantage of SMS/MB imaging is that there is no inherent SNR loss due to the acceleration gained by exciting multiple slices simultaneously [6, 7]. However, there is SNR loss based on the geometry of the receiver coil array, as it is used in the reconstruction. This loss can be further reduced using a technique called controlled aliasing while exciting the slices [6]. We have previously shown that SMS/MB imaging can be used in myocardial T_1 mapping to image three slices in a single breath-hold, significantly reducing the scan time [8]. However, this study had used a linear reconstruction algorithm without any regularization, leading to a reduced precision compared to imaging each slice independently [8].

In this work, we sought to develop a regularized SMS/MB reconstruction method that exploits two types of interpolation strategies in k-space, while allowing for further reduction of noise. The proposed method is compared to various existing techniques, and is shown to improve precision without compromising accuracy.

II. METHODS

A. Related Works

Slice-GRAPPA: Generalized Autocalibrating Partially Parallel Acquisitions (GRAPPA) is a k-space interpolation technique that uses information from multiple receiver coils [9]. For k-space data that is uniformly sub-sampled in-plane, GRAPPA estimates missing k-space points using linear shift-invariant convolutional kernels applied to acquired data points in a small neighborhood across all coils [9]. The weights of the convolutional kernels are determined from a fully sampled low-resolution calibration data, referred to as autocalibration signal (ACS).

Slice-GRAPPA extends GRAPPA reconstruction to SMS/MB imaging [10]. In slice-GRAPPA, different sets of GRAPPA kernels are applied to the SMS/MB data, which contains contribution from all slices, to synthesize individual k-spaces for each slice. Similar to GRAPPA, kernel weights are calculated from individual ACS data for each slice. The slice-GRAPPA equation can be written as follows [10]:

$$\kappa_{j,s}(k_x,k_y)=\sum_{c=1}^{N_c}\sum_{b_x=-B_x}^{B_x}\sum_{b_y=-B_y}^{B_y} w_{j,s,c}^{b_x,b_y}\cdot \kappa_c^{MB}(k_x-b_x\Delta k_x,k_y-b_y\Delta k_y) \quad (1)$$

where $\kappa_{j,s}$ is the k-space data of the j^{th} coil of he s^{th} slice, κ_c^{MB} is the SMS/MB k-space data of the c^{th} coil, B_x and B_y are specified by the kernel sizes, N_c is the number of coils, and $w_{j,s,c}^{b_x,b_y}$ are the pre-calibrated weights at locations b_x, b_y mapping from coil c of the SMS/MB data to the j^{th} coil of slice s. Note that slice-GRAPPA generates an entirely new k-space for each coil of a particular slice whereas in conventional

GRAPPA only the unacquired k-space points are synthesized. While slice-GRAPPA is efficient in removing aliasing artifacts, it is a linear method that suffers from noise amplification based on the coil geometry [11].

SMS/MB imaging can also be used in conjunction with in-plane acceleration to achieve higher acceleration rates. In this case, a typical approach is to use slice-GRAPPA to synthesize sub-sampled data for each slice, which is then reconstructed using conventional GRAPPA [8, 10].

Slice-SPIRiT: Iterative Self-consistent Parallel Imaging Reconstruction (SPIRiT) is another reconstruction technique that relies on k-space interpolation that jointly enforces consistency with acquired data, and consistency among the data from multiple coils [12]. Using ACS data, SPIRiT estimates a convolutional kernel, denoted by the matrix $\mathbf{G}$, which includes contribution from all points, both acquired and missing, across all coils around a given k-space point. Then the SPIRiT reconstruction solves

$$\arg\min_{\boldsymbol{\kappa}} ||\mathbf{P}_\Omega \boldsymbol{\kappa} - \mathbf{y}||_2^2 + \mu||\mathbf{G}\boldsymbol{\kappa} - \boldsymbol{\kappa}||_2^2, \tag{2}$$

where $\mathbf{y}$ is the acquired k-space data, $\boldsymbol{\kappa}$ is the k-space data across all coils, $\mathbf{P}_\Omega$ is a sub-sampling operator that samples the k-space data at locations specified by Ω, and μ is a weight term. Note the first ℓ_2 term in the objective function enforces consistency with the acquired data, while the second ℓ_2 term essentially states that the effect of the SPIRiT convolution on k-space data should enforce self-consistency across multiple coils. The main advantages of the SPIRiT formulation is its ability to work with arbitrary sub-sampling patterns, and not just uniform ones like GRAPPA, as well as the ease of incorporating additional regularizers (e.g. based on sparsity or low-rank properties) in the objective function [12].

SPIRiT has recently been extended to SMS by enforcing self-consistency for individual slices [13, 14]. This technique, called SMS-L1-SPIRiT, solves an objective function of the form:

$$\begin{aligned}\arg\min_{\boldsymbol{\kappa}_1,\cdots,\boldsymbol{\kappa}_n} &||\mathbf{P}_\Omega(\boldsymbol{\kappa}_1 + \cdots + \boldsymbol{\kappa}_n) - \boldsymbol{\kappa}_{MB}||_2^2 \\ &+ \sum_i \beta_i||\mathbf{G}\boldsymbol{\kappa}_i - \boldsymbol{\kappa}_i||_2^2 + \sum \sigma_i \Psi(\boldsymbol{\kappa}_i),\end{aligned} \tag{3}$$

where $\boldsymbol{\kappa}_{MB}$ is the acquired MB data across all coils in k-space, $\boldsymbol{\kappa}_i$ is the k-space data across all coils of the i^{th} slice, $\mathbf{P}_\Omega$ is a sub-sampling operator as previously defined, Ψ is a regularizer, which was taken as the time-domain finite difference of each coil image in [13].

B. Slice MB-SPIRiT/GRAPPA

In this work, we seek to use the advantages of slice-GRAPPA in removing aliasing artifacts, and of SPIRiT in enforcing self-consistency and enabling the use of regularization. Thus, our proposed method, called MB-SPIRiT/GRAPPA, combines these two k-space reconstruction strategies, by solving the following objective function:

$$\begin{aligned}\arg\min_{\boldsymbol{\kappa}_1,\ldots,\boldsymbol{\kappa}_n} &||\mathbf{P}_\Omega(\boldsymbol{\kappa}_1 + \cdots + \boldsymbol{\kappa}_n) - \boldsymbol{\kappa}_{MB}||_2^2 \\ &+ \mu\left|\left|\mathbf{G_{MB}}\boldsymbol{\kappa}_{MB} - \begin{bmatrix}\boldsymbol{\kappa}_1 \\ \vdots \\ \boldsymbol{\kappa}_n\end{bmatrix}\right|\right|_2^2 \\ &+ \sum_{i=1}^{n} \beta_i||\mathbf{G_i}\boldsymbol{\kappa}_i - \boldsymbol{\kappa}_i||_2^2 + \sum_{i=1}^{n} \sigma_i \Psi(\mathbf{E}_i\boldsymbol{\kappa}_i)\end{aligned} \tag{4}$$

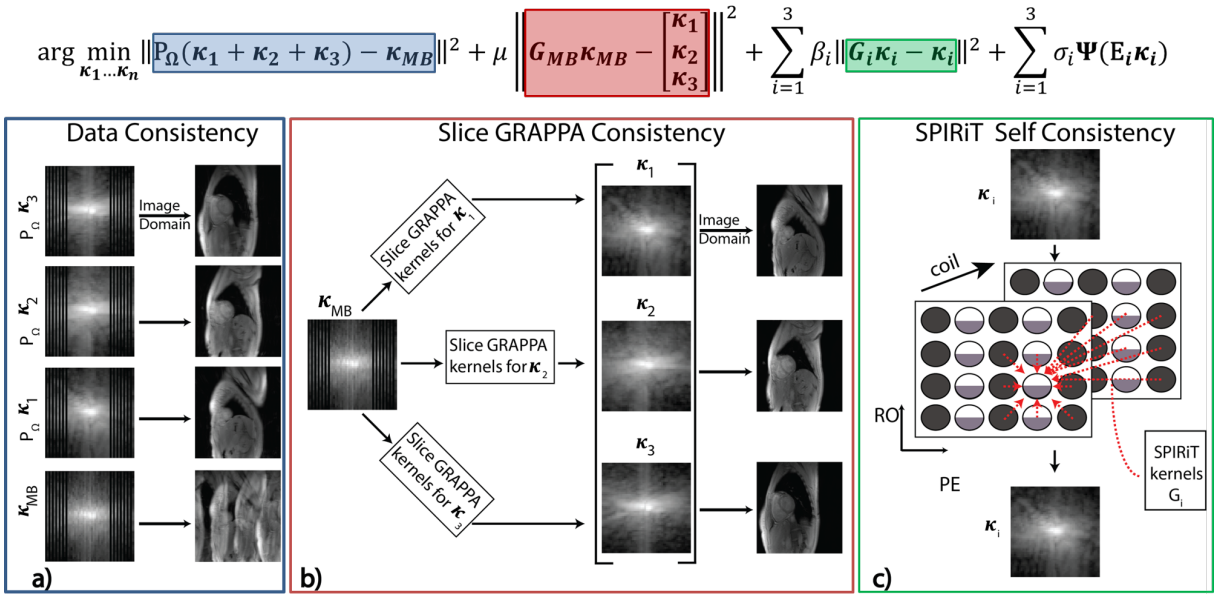

Fig. 1. A visual schematic of the objective function in Equation (4) for the proposed slice MB-SPIRiT/GRAPPA method. a) Data consistency term, enforces consistency with acquired k-space data, b) Slice-specific GRAPPA kernels provide a noisy but reliable estimate of the individual k-space slices, c) Further reduction in noise is achieved by introducing coil self-consistency terms, as in the SPIRiT framework. An MB factor of $n = 3$ is shown, and the regularization term is not depicted.

where $\mathbf{P}_\Omega$ is a sub-sampling operator as previously defined, $\boldsymbol{\kappa}_{MB}$ is the acquired MB data across all coils in k-space, $\boldsymbol{\kappa}_i$ is the k-space data across all coils of the i^{th} slice, $\mathbf{G_{MB}}$ is the slice-GRAPPA operator as in Section II-A, $\mathbf{G_i}$ is the SPIRiT self-consistency operator for the i^{th} slice, Ψ is a regularizer, μ, β_i and σ_i are weight terms. Finally, $\mathbf{E}_i$ is an operator that takes the inverse Fourier transform of all coil k-spaces in the i^{th} slice, and combines these images into one image using coil sensitivity maps, which is referred to as the SENSE-1 combination [11]. A schematic description of the data consistency (first term), slice-GRAPPA consistency (second term) and SPIRiT coil self-consistency (third term) in Eq. 4 are depicted in Figure 1.

The objective function in Eq. 4 was solved using Alternating Direction Method of Multipliers (ADMM) with the following sub problems. At iteration t, the first sub problem is solved with respect to $\{\boldsymbol{\kappa}_1, \cdots, \boldsymbol{\kappa}_n\}$:

$$\begin{aligned}\arg \min_{\boldsymbol{\kappa}_1,\ldots,\boldsymbol{\kappa}_n} & ||\mathbf{P}_\Omega(\boldsymbol{\kappa}_1 + \cdots + \boldsymbol{\kappa}_n) - \boldsymbol{\kappa}_{MB}||_2^2 \\ & + \mu \left|\left| \mathbf{G_{MB}}\boldsymbol{\kappa}_{MB} - [\boldsymbol{\kappa}_1, \cdots, \boldsymbol{\kappa}_n]^T \right|\right|_2^2 \\ & + \sum_{i=1}^{n} \beta_i ||\mathbf{G_i}\boldsymbol{\kappa}_i - \boldsymbol{\kappa}_i||_2^2 \\ & + \sum_{i=1}^{n} \frac{\rho}{2} \left|\left| \mathbf{E_i}\boldsymbol{\kappa}_i - \mathbf{z}_i^{(t-1)} + \frac{\boldsymbol{\lambda}_i^{(t-1)}}{\rho} \right|\right|_2^2, \end{aligned} \tag{5}$$

where $\{\mathbf{z}_i^{(t-1)}\}$ are the $(t-1)^{\text{th}}$ iteration auxiliary variables, $\mathbf{z}_i$ introduced for constraining $\mathbf{E}_i\boldsymbol{\kappa}_i$, and $\{\boldsymbol{\lambda}_i\}$ are the dual variables. The update for $\{\mathbf{z}_i\}$ is given as

$$\arg \min_{\mathbf{z}_1,\ldots,\mathbf{z}_n} \sum_{i=1}^{n} \left[\left|\left| \mathbf{E}_i\boldsymbol{\kappa}_i^{(t)} - \mathbf{z}_i + \frac{\boldsymbol{\lambda}_i^{(t-1)}}{\rho} \right|\right|_2^2 + \frac{\sigma_i}{\rho}\Psi(\mathbf{z}_i) \right], \tag{6}$$

and the dual variables $\{\boldsymbol{\lambda}_i\}$ are updated as:

$$\boldsymbol{\lambda}_i^{(t)} = \boldsymbol{\lambda}_i^{(t-1)} + \rho(\mathbf{E_i}\boldsymbol{\kappa}_i^{(t)} - \mathbf{z_i}^{(t)}). \tag{7}$$

C. Imaging Experiments

Imaging was performed at 3T in a healthy subject with no contraindications to MRI. The study was approved by our institutional review board, and written informed consent was acquired before the study. SMS/MB imaging was acquired in a single breath-hold by using an electrocardiogram (ECG)-triggered saturation pulse-prepared heart rate independent inversion recovery (SAPPHIRE) sequence with Gradient Recalled Echo (GRE) imaging [8]. 3 slices were simultaneously imaged using MB excitation, where controlled aliasing (CAIPIRINHA) was utilized with $2\pi/3$ phase increments to reduce noise amplification [6]. In addition to MB excitation, an in-plane acceleration rate of 2 was utilized to acquire 15 images with different T_1 weightings in a single breath-hold. Other relevant imaging parameters include: field-of-view (FOV) = 320×320 mm^2, resolution = 2×2.1 mm^2, slice thickness = 10 mm. A separate free-breathing scan of three slices was acquired as calibration/ACS data for reconstruction with the same parameters but lower resolution = 2×5 mm^2.

For each of the three slices quantitative T_1 maps were generated using parameter fitting [8]. Quantitative analysis was performed for each of the 16 segments of the myocardium [15] using manually drawn regions of interest (ROIs). For each segment, the mean value in the ROI is reported as the estimated T_1 value, whereas the standard deviation in the ROI is reported as the spatial variability of the T_1 maps. This spatial variability is used as a surrogate for precision, since healthy people are not expected to have much variation in their native myocardial T_1 values beyond noise effects [3, 8].

D. Reconstruction

The acquired raw data with 3-fold SMS/MB and 2-fold in-plane accelerations were exported from the scanner to be processed offline. The slice-GRAPPA kernel, $\mathbf{G_{MB}}$, and the SPIRiT kernels, $\{\mathbf{G}_1, \mathbf{G}_2, \mathbf{G}_3\}$ were calibrated using the ACS data. A 5×5 kernel was used the former, and 7×7 kernel for the latter. The proposed technique was implemented with the following parameters: $\mu = 10^{-4}$ and $\beta_1 = \beta_2 = \beta_3 = 10^{-3}$. Reconstructions were performed both without regularization ($\sigma_1 = \sigma_2 = \sigma_3 = 0$) and with regularization ($\sigma_1 = \sigma_2 = \sigma_3 = 10^{-3}$). The regularizer was based on a locally low-rank

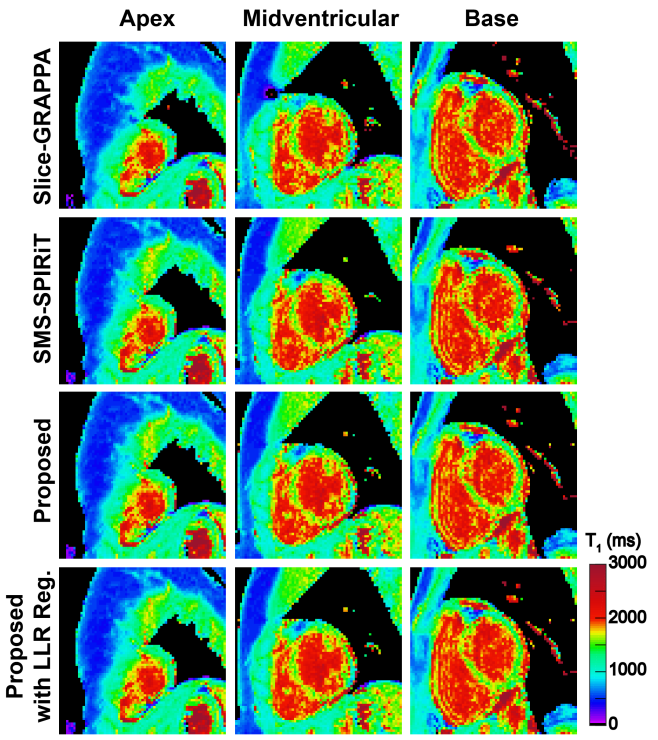

Fig. 2. T_1 maps of the three slices covering the heart, reconstructed using slice-GRAPPA (top), SMS-SPIRiT (second row) and the proposed slice MB-SPIRiT/GRAPPA without and with LLR regularization (third and fourth rows respectively). Among the non-regularized methods, visually improved spatial variability in the myocardium is observed using the proposed approach. Use of LLR regularization in the proposed method further leads to a modest reduction in spatial variability.

(LLR) constraint, which was shown to be effective in MR parameter mapping [16], as follows:

$$\Psi(\mathbf{x}) = \sum_k ||\mathbf{B}_k^b(\mathbf{x})||_*, \tag{8}$$

where $\mathbf{B}_k^b$ is an operator that extracts a $b \times b$ block, whose top-left corner is at pixel k, from each T_1-weighted image in the series, vectorizes these, and stacks them up into a $b^2 \times n_{T_1}$ matrix, where $b = 8$ and $n_{T_1} = 15$ in this study; and $||\cdot||_*$ is the nuclear norm. Eq. 6 was solved using singular value thresholding, where the thresholding parameter (i.e. σ_i/ρ) was set to 0.04 times the ℓ_∞ norm of the SENSE-1 image for the slice. All parameters (μ, β_i and σ_i) were empirically tuned.

For comparison, the slice-GRAPPA reconstruction followed by in-plane GRAPPA reconstruction as in [8] was implemented. In addition to the slice-GRAPPA kernel described previously, a 5×4 kernel for in-plane GRAPPA was utilized. Furthermore, SMS-SPIRiT was also implemented [13, 14] by setting $\mu = 0$ in Eq. 4, also with a 7×7 kernel size. All methods were implemented in MATLAB (Mathworks, Natick, MA). The run-time per iteration was 10 seconds for non-regularized SMS-SPIRiT and proposed method, and 30 seconds for the regularized versions.

III. RESULTS

Figure 2 shows the T_1 maps of the three slices, corresponding to the apex (left), midventricular (middle) and base (right) of the heart, reconstructed using slice-GRAPPA (top), SMS-SPIRiT (second row) and the proposed slice MB-SPIRiT/GRAPPA without and with regularization (third and fourth rows respectively). Visually improved spatial variability is observed with the proposed approach in the myocardium, especially in the septal region, and in the blood pools. Further gain is achieved with the regularized reconstruction.

Figure 3 shows bullseye representation of the 16 myocardial segments, for myocardial T_1 times and spatial variabilities (in ms) of the different reconstruction methods. All methods yield similar T_1 values ($< 1.5\%$ difference), indicating no bias in reconstruction. Among the non-regularized methods, the proposed slice MB-SPIRiT/GRAPPA technique shows the least spatial variability (167 ms), followed by SMS-SPIRiT (176 ms), and slice-GRAPPA (184 ms). A further reduction in spatial variability is achieved when using the proposed method with LLR regularization (157 ms).

IV. CONCLUSION

In this work, we proposed and evaluated a joint SPIRiT and slice-GRAPPA type reconstruction for SMS/MB imaging. The proposed MB-SPIRiT/GRAPPA reconstruction shows improved spatial variability compared to slice-GRAPPA and SMS-SPIRiT. Additionally, this method allows incorporation of regularizers for further reduction of reconstruction noise. Since our focus in this study was on the effective use of coil information, we used a previously established regularizer with a low weight as a proof-of-concept. Further optimization of the regularizer will be explored in future research. Further validation of the performance of the proposed method in a larger cohort will also be studied in future work.

ACKNOWLEDGMENT

This work was partially supported by NIH R00HL111410, NIH P41EB015894, NIH P41EB027061 and NSF CAREER CCF-1651825.

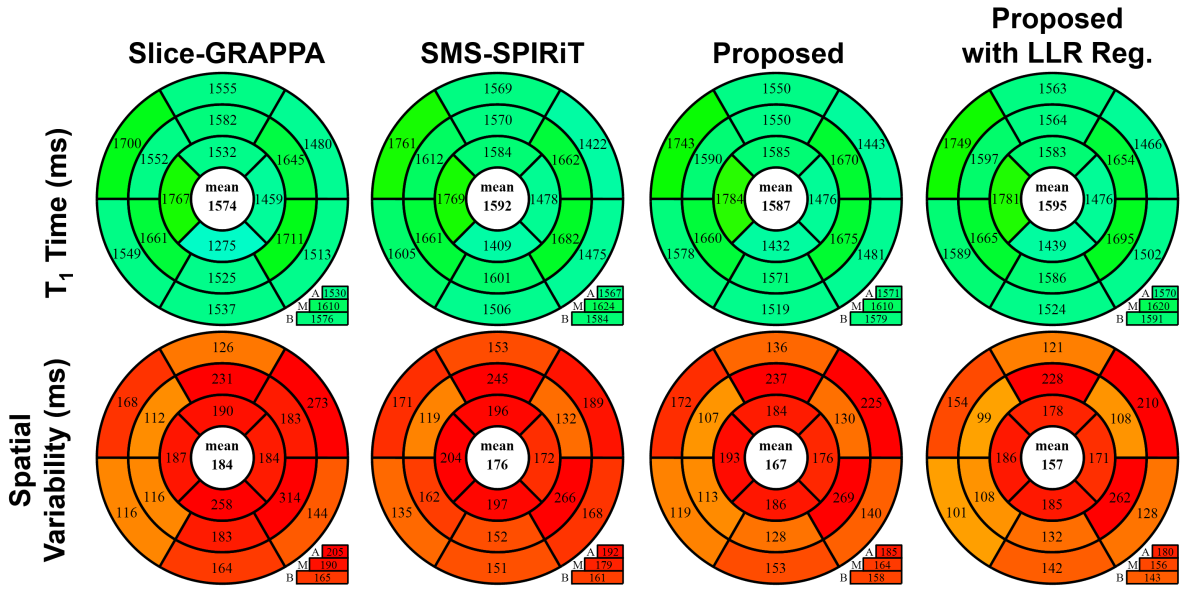

Fig. 3. Bullseye representation of myocardial T_1 times and T_1 spatial variability for slice-GRAPPA, SMS-SPIRiT, and the proposed slice MB-SPIRiT/GRAPPA without and with LLR regularization. Among non-regularized methods, slice MB-SPIRiT/GRAPPA shows the least spatial variability while maintaining comparable T_1 times. Slice MB-SPIRiT/GRAPPA with LLR regularization exhibits lower spatial variability compared to its corresponding non-regularized implementation. Mean T_1 times and T_1 spatial variability of the apical (A), midvenctricular (M) and basal (B) slices are also shown.

References

[1] J. R. Burt, S. L. Zimmerman, I. R. Kamel, M. Halushka, and D. A. Bluemke, "Myocardial T1 mapping: techniques and potential applications," *Radiographics*, vol. 34, no. 2, pp. 377–395, 2014.

[2] S. Giri, Y.-C. Chung, A. Merchant, G. Mihai, S. Rajagopalan, S. V. Raman, and O. P. Simonetti, "T2 quantification for improved detection of myocardial edema," *Journal of Cardiovascular Magnetic Resonance*, vol. 11, no. 1, p. 56, 2009.

[3] E. B. Schelbert and D. R. Messroghli, "State of the art: clinical applications of cardiac T_1 mapping," *Radiology*, vol. 278, no. 3, pp. 658–676, 2016.

[4] J. C. Moon, D. R. Messroghli, P. Kellman, S. K. Piechnik, M. D. Robson, M. Ugander, P. D. Gatehouse, A. E. Arai, M. G. Friedrich, S. Neubauer *et al.*, "Myocardial T1 mapping and extracellular volume quantification: a Society for Cardiovascular Magnetic Resonance (SCMR) and CMR Working Group of the European Society of Cardiology consensus statement," *Journal of Cardiovascular Magnetic Resonance*, vol. 15, no. 1, p. 92, 2013.

[5] D. J. Larkman, J. V. Hajnal, A. H. Herlihy, G. A. Coutts, I. R. Young, and G. Ehnholm, "Use of multicoil arrays for separation of signal from multiple slices simultaneously excited," *J Magn Reson Imaging*, vol. 13, no. 2, pp. 313–317, Feb 2001.

[6] F. A. Breuer, M. Blaimer, R. M. Heidemann, M. F. Mueller, M. A. Griswold, and P. M. Jakob, "Controlled aliasing in parallel imaging results in higher acceleration (CAIPIRINHA) for multi-slice imaging," *Magn Reson Med*, vol. 53, no. 3, pp. 684–691, Mar 2005.

[7] S. Moeller, E. Yacoub, C. A. Olman, E. Auerbach, J. Strupp, N. Harel, and K. Uğurbil, "Multiband multislice GE-EPI at 7 Tesla, with 16-fold acceleration using partial parallel imaging with application to high spatial and temporal whole-brain fMRI," *Magn Reson Med*, vol. 63, no. 5, pp. 1144–1153, 2010.

[8] S. Weingartner, S. Moeller, S. Schmitter, E. Auerbach, P. Kellman, C. Shenoy, and M. Akçakaya, "Simultaneous multislice imaging for native myocardial T_1 mapping: Improved spatial coverage in a single breath-hold," *Magn Reson Med*, vol. 78, no. 2, pp. 462–471, 08 2017.

[9] M. A. Griswold, P. M. Jakob, R. M. Heidemann, M. Nittka, V. Jellus, J. Wang, B. Kiefer, and A. Haase, "Generalized autocalibrating partially parallel acquisitions (GRAPPA)," *Magn Reson Med*, vol. 47, no. 6, pp. 1202–1210, 2002.

[10] K. Setsompop, B. A. Gagoski, J. R. Polimeni, T. Witzel, V. J. Wedeen, and L. L. Wald, "Blipped-controlled aliasing in parallel imaging for simultaneous multislice echo planar imaging with reduced g-factor penalty," *Magn Reson Med*, vol. 67, no. 5, pp. 1210–1224, May 2012.

[11] K. P. Pruessmann, M. Weiger, M. B. Scheidegger, and P. Boesiger, "SENSE: Sensitivity encoding for fast MRI," *Magnetic Reson Med*, vol. 42, no. 5, pp. 952–962, 1999.

[12] M. Lustig and J. M. Pauly, "SPIRiT: Iterative self-consistent parallel imaging reconstruction from arbitrary k-space," *Magn Reson Med*, vol. 64, no. 2, pp. 457–471, Aug 2010.

[13] Y. Yang, C. H. Meyer, F. H. Epstein, C. M. Kramer, and M. Salerno, "Whole-heart spiral simultaneous multi-slice first-pass myocardial perfusion imaging," *Magn Reson Med*, Oct 2018.

[14] S. Rapacchi, T. Troalen, Z. Bentatou, M. Quemeneur, M. Guye, M. Bernard, A. Jacquier, and F. Kober, "Simultaneous multi-slice cardiac cine with Fourier-encoded self-calibration at 7 Tesla," *Magn Reson Med*, 2018.

[15] AHA Writing Group on Myocardial Segmentation and Registration for Cardiac Imaging, "Standardized myocardial segmentation and nomenclature for tomographic imaging of the heart: A statement for healthcare professionals from the cardiac imaging committee of the council on clinical cardiology of the American Heart Association," *Circulation*, vol. 105, pp. 539–542, 2002.

[16] T. Zhang, J. M. Pauly, and I. R. Levesque, "Accelerating parameter mapping with a locally low rank constraint," *Magn Reson Med*, vol. 73, no. 2, pp. 655–661, Feb 2015.